

# Simple and efficient algorithms for training machine learning potentials to force data

Justin S. Smith,<sup>1</sup> Nicholas Lubbers,<sup>2</sup> Aidan P. Thompson,<sup>3</sup> and Kipton Barros<sup>1, a)</sup>

<sup>1)</sup>*Theoretical Division and CNLS, Los Alamos National Laboratory, Los Alamos, New Mexico 87545, USA*

<sup>2)</sup>*Computer, Computational, and Statistical Sciences Division, Los Alamos National Laboratory, Los Alamos, New Mexico 87545, USA*

<sup>3)</sup>*Center for Computing Research, Sandia National Laboratories, Albuquerque, New Mexico 87185, USA*

Machine learning models, trained on data from *ab initio* quantum simulations, are yielding molecular dynamics potentials with unprecedented accuracy. One limiting factor is the quantity of available training data, which can be expensive to obtain. A quantum simulation often provides all atomic forces, in addition to the total energy of the system. These forces provide much more information than the energy alone. It may appear that training a model to this large quantity of force data would introduce significant computational costs. Actually, training to all available force data should only be a few times more expensive than training to energies alone. Here, we present a new algorithm for efficient force training, and benchmark its accuracy by training to forces from real-world datasets for organic chemistry and bulk aluminum.

## I. INTRODUCTION

Machine learning (ML) is driving the development of next-generation interatomic potentials. By training the ML model to a large and diverse dataset of *ab initio* quantum simulations, one aims to build a low-cost, high-fidelity emulator, valid over a wide space of atomic configurations. For example, such ML potentials can be used as the basis for large scale molecular dynamics simulations with unprecedented accuracy.<sup>1,2</sup>

The reference data is generated by approximate solution to the Schrödinger equation, typically using a tool such as density functional theory (DFT). Under the Born Oppenheimer approximation, nuclei are treated classically. Each reference calculation takes as input the atomic configuration (nuclei positions and species) and outputs total energy  $E$ . Often, once the total energy has been computed, forces  $\mathbf{f}_i = -\partial E/\partial \mathbf{r}_i$  for *all* atoms  $i$  can be produced, at minimal additional cost. If possible to acquire, these forces provide highly valuable training data for the ML model. For a system with  $N$  atoms, the collection of force components comprise  $3N$  times more data than the energy scalar.

The ML model predicts a potential energy surface  $\hat{E}$  that is hopefully a good approximation to the true energy  $E$ , even for configurations outside the training set. To maximize generality, it is natural to train the ML model such that its predicted energy  $\hat{E}$  and forces  $\hat{\mathbf{f}}_i = -\partial \hat{E}/\partial \mathbf{r}_i$  agree with reference data. It might appear that incorporating a large quantity of force data into the training procedure would incur a large increase in computational cost. Here, we show otherwise. In the context of neural networks (or more generally, any method based on gradient-based optimization of a loss function) one can train on energy *and* force data at a cost comparable to training on

the energy data alone. Readers familiar with ML frameworks (ML-F) such as PyTorch<sup>3</sup> or TensorFlow<sup>4</sup> may recognize the above statement as self-evident. The principle of reverse-mode automatic differentiation (backpropagation) *guarantees* that the gradient of a scalar loss function can be efficiently calculated, *independent* of the number of gradient components.<sup>5</sup> The backpropagation procedure effectively requires tracing backward through all computational steps that were used to calculate the loss. An ML-F will automatically execute this procedure to produce the full gradient.

Prototyping new ML codes inside an ML-F is an obvious choice. However, there remain several reasons why certain *production* ML codes may wish to avoid use of an ML-F. An obvious one is that it can be difficult to port existing codes into the constrained context of an ML-F. Another reason may be memory constraints. By design, the ML-F needs to track every computational operation, recording all associated data, in order to backpropagate. It is often possible to design alternative algorithms to calculate a gradient, for which memory requirements are significantly reduced.<sup>6</sup> Finally, there is a question of performance. Codes may wish to avoid an ML-F if they require types of calculations that are not easily expressible in terms of high-level tensor operations. Although next-generation ML-Fs such as JAX<sup>7,8</sup> and Zygote<sup>9</sup> enable backpropagation through nearly arbitrary Python or Julia code, costs arising from automated tracing seem unavoidable.

Our main contribution is a simple algorithm to efficiently calculate the full gradient of a loss function that directly incorporates force data. This algorithm works with or *without* an ML-F, and so remains fully general. In particular, the method can be applied to any existing neural network code that was designed to train to energy data, including AENet,<sup>10</sup> N2P2,<sup>11,12</sup> ANI,<sup>13</sup> and PINN.<sup>14</sup>

In a practical implementation, the cost to evaluate the loss gradient may be about 3 times the cost to predict all

<sup>a)</sup>Electronic mail: kbarros@lanl.gov

forces, independent of the number of atoms and number of model parameters.

## II. EVALUATING THE LOSS GRADIENT

### A. Problem statement

Our context is as follows: We seek to optimize (i.e., train) model parameters  $\theta$  such that the ML-predicted energy function  $\hat{E}_\theta[\mathbf{r}]$  minimizes a loss function,

$$\mathcal{L} = c_1 \mathcal{L}_{\text{energy}} + c_2 \mathcal{L}_{\text{force}} + \mathcal{L}_{\text{reg}}.$$

The terms

$$\begin{aligned} \mathcal{L}_{\text{energy}} &= \frac{1}{2} \langle (\hat{E} - E)^2 \rangle \\ \mathcal{L}_{\text{force}} &= \frac{1}{2} \left\langle \sum_{i \in \text{atoms}} |\hat{\mathbf{f}}_i - \mathbf{f}_i|^2 \right\rangle, \end{aligned} \quad (1)$$

constrain the model predictions  $\hat{E}$  and  $\hat{\mathbf{f}}_i$  to match reference energy and force data. Angle brackets  $\langle \cdot \rangle$  denote an average over the dataset. The final term  $\mathcal{L}_{\text{reg}}$  is a placeholder for various possible model regularization terms. Coefficients  $c_1$  and  $c_2$  are fixed prior to training.

Optimization of model parameters  $\theta$  typically involves some variant of stochastic gradient descent, which requires the loss gradient  $\nabla_\theta \mathcal{L}$ , or an approximation to it. A modern neural network will typically have  $10^4$  or more scalar components in  $\theta$  and, therefore, in  $\nabla_\theta \mathcal{L}$ . It is essential to calculate this full loss gradient efficiently. One can handle  $\nabla_\theta \mathcal{L}_{\text{energy}}$  with ordinary backpropagation. Calculating  $\nabla_\theta \mathcal{L}_{\text{force}}$ , however, presents an interesting challenge.

To simplify notation, let us focus attention on a single data point, e.g. a single DFT calculation. For a system with  $N$  atoms, we define

$$L = \frac{1}{2} \sum_{i=1}^N |\hat{\mathbf{f}}_i - \mathbf{f}_i|^2. \quad (2)$$

The target  $\nabla_\theta \mathcal{L}_{\text{force}}$  can be calculated by averaging  $\nabla_\theta L$  over all data points.

Our focus, then, is efficient calculation of  $\nabla_\theta L$ . This appears difficult, because  $L$  already incorporates derivatives of the ML potential, via its dependence on

$$\hat{\mathbf{f}}_i = -\partial \hat{E} / \partial \mathbf{r}_i. \quad (3)$$

Naïve expansion indicates that  $\nabla_\theta L$  involves all *second* derivatives  $\partial^2 \hat{E} / \partial \mathbf{r}_i \partial \theta_j$ . Fortunately, it is not necessary to evaluate all these components individually. Below, we demonstrate two methods to efficiently calculate  $\nabla_\theta L$  at a cost comparable to the calculation of  $L$  alone.

### B. Approach 1: Iterated backpropagation

As previously mentioned, ML frameworks (ML-F) such as PyTorch or TensorFlow offer an efficient algorithm to calculate the full gradient  $\nabla_\theta L$ . This calculation happens as follows. Using primitives provided by the ML-F, the user writes a code to calculate energy  $\hat{E}$  and the loss  $L$  in terms of  $\hat{E}$  and  $\hat{\mathbf{f}}$ . The ML-F will first execute the code to calculate  $\hat{E}[\mathbf{r}]$ , tracing all dependencies on the atomic configuration  $\mathbf{r}$  and the model parameters  $\theta$ . Operating backward on that trace, the ML-F then efficiently calculates all forces  $\hat{\mathbf{f}}$ . Once these forces are known, the ML-F can calculate the loss  $L$ . Throughout the entire calculation of  $L$  (including the backpropagation phase to calculate  $\hat{\mathbf{f}}$ ), *tracing remains active*. A second backpropagation step can then be performed, this time to calculate the full gradient  $\nabla_\theta L$ . We emphasize that the calculation of  $\nabla_\theta L$  involves backpropagating through the backpropagation step used to calculate  $\hat{\mathbf{f}}$ . In other words, calculation of  $\nabla_\theta L$  effectively requires *four* traversals of the computational graph to calculate  $\hat{E}[\mathbf{r}]$ . Remarkably, these steps are completely automated by the ML-F. Implementing iterated backpropagation without the help of an ML-F would be a daunting task.

Many popular ML potentials have been written in an ML-F, for which the iterated backpropagation strategy is a natural fit.<sup>15–22</sup>

### C. Approach 2: Directional derivative of the energy gradient

Here we demonstrate that it is possible to efficiently calculate the full gradient  $\nabla_\theta L$ , even without the aid of an ML-F. This algorithm should be applicable to any existing neural network code. Our *only assumption* is that subroutines are available to efficiently calculate the energy  $\hat{E}$ , as well as its two gradients,  $\partial \hat{E} / \partial \mathbf{r}_i$  and  $\nabla_\theta \hat{E}$ .<sup>23</sup>

The error in the force predictions are readily calculated,

$$\mathbf{g}_i[\mathbf{r}] = \hat{\mathbf{f}}_i[\mathbf{r}] - \mathbf{f}_i[\mathbf{r}]. \quad (4)$$

The loss gradient may then be written as

$$\nabla_\theta L = \nabla_\theta \frac{1}{2} \sum_{i=1}^N |\mathbf{g}_i|^2 = \sum_{i=1}^N \mathbf{g}_i \cdot \nabla_\theta \hat{\mathbf{f}}_i. \quad (5)$$

In the second step we used the fact that  $\mathbf{f}_i$  is ground truth data, independent of model parameters  $\theta$ . Applying the definition  $\hat{\mathbf{f}}_i = -\partial \hat{E} / \partial \mathbf{r}_i$  and commuting derivatives yields

$$\nabla_\theta L = - \sum_{i=1}^N \mathbf{g}_i \cdot \frac{\partial}{\partial \mathbf{r}_i} (\nabla_\theta \hat{E}). \quad (6)$$

Naïvely, one might consider evaluating  $\nabla_\theta L$  by finite differencing on all  $N$  positions  $\mathbf{r}_i$  individually. There is a

better algorithm, however, which avoids introducing a factor of  $N$  into the computational cost.

The idea is to interpret  $\mathbf{g} = [\mathbf{g}_1, \mathbf{g}_2 \dots \mathbf{g}_N]$  as a  $3N$ -dimensional vector in the space of all atomic coordinates, and  $\frac{\partial}{\partial \mathbf{r}} = [\frac{\partial}{\partial \mathbf{r}_1}, \frac{\partial}{\partial \mathbf{r}_2}, \dots \frac{\partial}{\partial \mathbf{r}_N}]$  as the gradient vector in this space. In this language, the loss gradient ( $\nabla_{\theta} L$ ) may be viewed as a *directional derivative* of the energy gradient ( $\nabla_{\theta} \hat{E}$ ) along the direction of force errors ( $\mathbf{g}$ ). Central differencing gives,

$$\nabla_{\theta} L \approx \tilde{\nabla}_{\theta} L = -\frac{\nabla_{\theta} \hat{E}[\mathbf{r}_+] - \nabla_{\theta} \hat{E}[\mathbf{r}_-]}{2\eta}, \quad (7)$$

where  $\mathbf{r}_+$  and  $\mathbf{r}_-$  denote new configurations in which each atom is slightly perturbed,

$$(\mathbf{r}_{\pm})_i = \mathbf{r}_i \pm \eta \mathbf{g}_i. \quad (8)$$

In Eq. (7),  $\mathbf{r}_+$  and  $\mathbf{r}_-$  are to be held fixed with respect to variations in  $\theta$  (namely, we *impose*  $\nabla_{\theta} \mathbf{r}_{\pm} = 0$ ). Models  $\hat{E}$  are typically designed to be smooth, so Eq. (7) is valid to order  $\mathcal{O}(\eta^2)$ . The ‘‘small’’ parameter  $\eta$  has units of length per force. Its selection will be discussed below.

Combining the above results, our method can be summarized as follows:

#### Steps for efficient evaluation of loss gradient

1. For a given atomic configuration  $\mathbf{r}$ , calculate all predicted forces  $\hat{\mathbf{f}}$ , and associated force errors,  $\mathbf{g} = \hat{\mathbf{f}} - \mathbf{f}$ .
2. Generate slightly perturbed atomic configurations  $\mathbf{r}_{\pm} = \mathbf{r} \pm \eta \mathbf{g}$
3. Evaluate the full energy gradient  $\nabla_{\theta} \hat{E}$  at new configurations  $\mathbf{r}_+$  and  $\mathbf{r}_-$ .
4. Use central differences, Eq. (7), to approximate  $\nabla_{\theta} L = \tilde{\nabla}_{\theta} L + \mathcal{O}(\eta^2)$ .

In total, this recipe requires calculating forces  $\hat{\mathbf{f}}$  and two additional energy gradients,  $\nabla_{\theta} \hat{E}[\mathbf{r}_+]$ , and  $\nabla_{\theta} \hat{E}[\mathbf{r}_-]$ . Compared to the method of Sec. II B, less memory is required because here we avoid iterated backpropagation.

Equation (7) may be interpreted as an approximation to Pearlmutter’s algorithm for efficient multiplication by the Hessian.<sup>24</sup> In Pearlmutter’s version, the  $\eta \rightarrow 0$  limit is taken, avoiding numerical errors due to finite differencing. This can be achieved using the method of *forward mode* automatic differentiation.<sup>5</sup> Specifically, the code to calculate  $\nabla_{\theta} \hat{E}$  should be transformed into one that operates on so-called dual numbers, which are designed to track infinitesimal perturbations. Unlike reverse mode autodiff, the forward mode version requires no tracing.

Existing neural network codes are unlikely to support dual numbers, so we instead advocate the central difference approximation of Eq. (7). The next section will indicate that numerical errors can be quite small.

### III. MINIMIZING NUMERICAL ERROR

#### A. Scaling the finite differencing parameter

The finite differencing scheme of Eq. (7) requires selection of a sufficiently small parameter  $\eta$ . Since  $\eta$  actually carries dimensions, it is natural to factorize

$$\eta = \epsilon a_0 / g_0, \quad (9)$$

where  $a_0$  is a characteristic length scale, and  $g_0$  is a characteristic scale associated with errors in the force predictions,  $\mathbf{g}$ . The small dimensionless parameter  $\epsilon$  should be selected according to floating point round-off considerations, as will be discussed below.

For simplicity, we fix  $a_0 = \text{\AA}$ . The characteristic scale  $g_0$  should vary according to the accuracy of the model’s force predictions, as applied to a particular system. A reasonable choice is

$$g_0 = \max_{i=1 \dots N} |\mathbf{g}_i|, \quad (10)$$

selected on a per system basis.

#### B. Two measures of error

A direct error measure for the finite differencing scheme of Eq. (7) is,

$$\text{Err}[\tilde{\nabla} L] = \frac{|\tilde{\nabla}_{\theta} L - \nabla_{\theta} L|}{|\nabla_{\theta} L|}. \quad (11)$$

The bars  $|\cdot|$  denote an  $L_2$  norm, to be taken over all  $\theta$  components, and all points in the dataset (e.g. all DFT calculations).

Ideally, one would like to know how floating point round-off errors contribute to  $\text{Err}[\tilde{\nabla} L]$ . In applications, it may be infeasible to calculate  $\nabla_{\theta} L$  to full precision, and we therefore will not know the true numerical error in  $\tilde{\nabla}_{\theta} L$ . To circumvent this limitation, it will be useful to introduce a second error measure that can be used as a proxy for  $\text{Err}[\tilde{\nabla} L]$ .

Removing the gradient operator  $\nabla_{\theta}$  from the right hand side of Eq. (7) yields a new finite difference approximation,

$$\frac{\hat{E}[\mathbf{r}_+] - \hat{E}[\mathbf{r}_-]}{2\eta} \approx \sum_i \mathbf{g}_i \cdot \frac{\partial \hat{E}}{\partial \mathbf{r}_i}, \quad (12)$$

again valid to order  $\mathcal{O}(\eta^2)$ . Using  $L = \frac{1}{2} \sum_i \mathbf{g}_i \cdot (\hat{\mathbf{f}}_i - \mathbf{f}_i)$ , we find that

$$L \approx \tilde{L} = -\frac{\hat{E}[\mathbf{r}_+] - \hat{E}[\mathbf{r}_-]}{4\eta} - \frac{1}{2} \sum_i \mathbf{g}_i \cdot \mathbf{f}_i. \quad (13)$$

This suggests a new error measure

$$\text{Err}[\tilde{L}] = \frac{|\tilde{L} - L|}{|L|}, \quad (14)$$

which should reflect  $\text{Err}[\tilde{\nabla}L]$ , insofar as the finite difference approximations Eqs. (7) and (13) have comparable round-off errors. Below we present evidence to this effect.

Because the reference loss  $L$  is generally available, the error measure  $\text{Err}[\tilde{L}]$  can be calculated to high precision with existing codes.

### C. Empirical error measurements

Here we demonstrate a numerical procedure for selecting the dimensionless parameter  $\epsilon$ , which fixes  $\eta$  via Eq. (9).

Our intention is that the approximate loss gradient  $\tilde{\nabla}_\theta L$  will ultimately be used to enable a gradient descent training procedure, for which the ML model will have a highly nonlinear dependence on its model parameters  $\theta$ . In this subsection, however, we consider the simpler context of a linear regression model so that it becomes possible to precisely evaluate the effects of floating point round-off on  $\text{Err}[\tilde{\nabla}L]$ . Local energy contributions will be modeled as  $\hat{E} = \sum_j \theta_j B_j$ , where  $\theta_j$  are fitting coefficients and  $B_j$  serve as descriptors of each local atomic environment. For concreteness, we select a SNAP potential for tantalum, and use its corresponding dataset.<sup>25,26</sup> In SNAP, the descriptors  $B_j$  are bispectrum coefficients. The dataset consists of 362 different configurations, sampled from both crystal and liquid phases.<sup>26</sup> System sizes in this dataset range from 2 to 100 tantalum atoms. Reference energy and force data were computed with DFT.

In the context of an ML training procedure, we must account for the fact that the parameters  $\theta$  will be rapidly evolving. Ideally,  $\tilde{\nabla}_\theta L$  should remain a good approximation to  $\nabla_\theta L$  for *arbitrary* model parameters  $\theta$ . Therefore, in addition to the trained SNAP potential, we also consider an *untrained* model, for which we randomize the model parameters  $\theta_j$  according to the Kaiming initialization procedure.<sup>27</sup>

Figure 1 shows empirical measurements of errors associated with the approximation  $\tilde{\nabla}_\theta L \approx \nabla_\theta L$ , for various values of the dimensionless finite differencing parameter  $\epsilon$ . Importantly, a *single* value,  $\epsilon \approx 10^{-5}$ , is observed to minimize the error for both trained and untrained models. This optimal  $\epsilon$  balances the  $\mathcal{O}(\epsilon^2)$  central differencing error with the floating point round-off error. For this calculation, we used 64-bit (double-precision) floating point accuracy, for which the 53 bit significand corresponds to approximately 16 digits of precision. Here, the proper selection of  $\epsilon$  yields about 9 digits of accuracy in estimates  $\tilde{\nabla}_\theta L$  of the loss gradient,  $\nabla_\theta L$ , which is more than sufficient for neural network training.

Figure 1 actually reports our *two* measures of error, namely  $\text{Err}[\tilde{\nabla}L]$  and  $\text{Err}[\tilde{L}]$ . Recall that the former represents the true error in the approximation  $\tilde{\nabla}_\theta L \approx \nabla_\theta L$ , and the latter is intended as a proxy for the true error. Our results indicate that, indeed,  $\text{Err}[\tilde{\nabla}L]$  and  $\text{Err}[\tilde{L}]$  are of comparable scale. When moving to real-world neural network codes,  $\text{Err}[\tilde{L}]$  will be easy to directly measure.

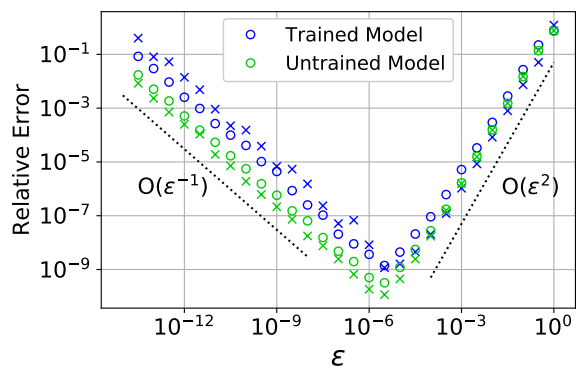


Figure 1. Relative error in the finite difference estimates of  $\nabla_\theta L$  for trained and untrained SNAP potentials of tantalum. Circles denote the true error  $\text{Err}[\tilde{\nabla}L]$ , and crosses denote its proxy  $\text{Err}[\tilde{L}]$ . Central differencing errors formally scale as  $\mathcal{O}(\epsilon^2)$  in the small parameter  $\epsilon$ . Accounting for double-precision round-off errors, the choice  $\epsilon \approx 10^{-5}$  yields the smallest errors for both model types (under both error measures).

Our general recommendation is to select  $\epsilon$  to minimize  $\text{Err}[\tilde{L}]$ . The results of Fig. 1 indicate that this choice of  $\epsilon$  will yield a quality approximation  $\tilde{\nabla}_\theta L \approx \nabla_\theta L$ , even under significant variations to the model parameters  $\theta$ .

The scaling relations of Eqs. (9) and (10) are crucial for ensuring that  $\epsilon$  is roughly invariant to model quality. In particular, as the model improves, the typical force errors  $\mathbf{g} = \hat{\mathbf{f}} - \mathbf{f}$  decrease, and the finite differencing parameter  $\eta$  should *increase*, so that the characteristic atomic displacements  $\mathbf{r}_\pm - \mathbf{r} = \pm \eta \mathbf{g}$  of Eq. (8) have a roughly invariant scale. Appendix A demonstrates the importance of accounting for these scaling relationships.

## IV. BENEFITS OF FORCE TRAINING

Our initial motivation for developing the force training scheme of Sec. II C was to support ANAKIN-ME (ANI) models.<sup>13</sup> ANI is a variant of the Behler Parrinello neural network architecture.<sup>28</sup> The Neurochem implementation of ANI is written in highly optimized C++/CUDA code,<sup>29</sup> and does not use an ML framework such as PyTorch or TensorFlow. Applied to a recently developed aluminum potential, NeuroChem can calculate 1,000 atomic forces in about 20 ms, running on a single modern GPU (Nvidia RTX 2080 Ti).<sup>1</sup> For comparison, TorchANI is a recent reimplementation of ANI in PyTorch, designed for flexibility.<sup>21</sup> TorchANI makes prototyping new model variants much easier, but is up to an order of magnitude slower than NeuroChem. Whereas TorchANI can use the iterated backpropagation scheme of Sec. II B, the optimized NeuroChem implementation cannot. Fortunately, the method presented in Sec. II C allows NeuroChem to also train to force data in a very efficient manner.

	ANI-1x (chem.)	ANI-Al (alum.)
<u>Training on energy data only</u>		
Energy RMSE	$1.48 \pm 0.01 \frac{\text{kcal}}{\text{mol}}$	$4.38 \pm 0.45 \frac{\text{meV}}{\text{atom}}$
Force RMSE	$4.12 \pm 0.02 \frac{\text{kcal}}{\text{mol \AA}}$	$0.39 \pm 0.05 \frac{\text{eV}}{\text{\AA}}$
<u>Training on energy <i>and</i> force data</u>		
Energy RMSE	<b><math>1.38 \pm 0.01 \frac{\text{kcal}}{\text{mol}}</math></b>	<b><math>1.88 \pm 0.2 \frac{\text{meV}}{\text{atom}}</math></b>
Force RMSE	<b><math>2.78 \pm 0.014 \frac{\text{kcal}}{\text{mol \AA}}</math></b>	<b><math>0.045 \pm 0.001 \frac{\text{eV}}{\text{\AA}}</math></b>

Table I. Root-mean-squared-errors (RSME) for neural network energy and force predictions. Models were trained to the ANI-1x and ANI-Al datasets for organic chemistry and bulk aluminum, respectively.

We demonstrate the value of training to force data by benchmarking on two real-world datasets. The first, ANI-1x, includes about 5M DFT calculations on single organic molecules (elements C, H, N, and O, with a mean molecule size of about 15 atoms), over a broad range of conformations.<sup>30</sup> The second, ANI-Al, includes about 6,000 DFT calculations on bulk aluminum, in various melt and crystal configurations, each containing about 100 to 200 atoms.<sup>1</sup> Both datasets were generated automatically using an active learning procedure, which aims to maximize the diversity of the atomic configurations.<sup>31</sup> For each of the two datasets, we trained two ML potentials. The first potential was trained to energy data only, and the second potential was trained to both energy *and* force data. We employ ensemble averaging to reduce model variance; each ML potential actually consists of eight ANI neural networks, differing only in the random initialization of their weights prior to training. Model details and training procedures are described in previous work.<sup>1,31</sup>

The force training scheme of IIC requires selection of a finite differencing parameter  $\eta$  via the dimensionless number  $\epsilon$ . The NeuroChem implementation uses a careful mix of 32 bit and 64 bit floating point precision, and the optimal choice of  $\epsilon$  would be difficult to guess *a priori*. We selected  $\epsilon = 10^{-3}$  to approximately minimize  $\text{Err}[\tilde{L}]$ , and found that this choice yields reasonable estimates of the loss gradient  $\nabla_{\theta} L$  throughout the training procedure.

Table 1 shows the resulting errors in energy and force predictions, as measured on held-out test data. Because the natural energy units vary according to domain, we use kcal/mol for the ANI-1x dataset (organic chemistry) and eV for the ANI-Al data (bulk aluminum).

For ANI-1x, including force data into the training procedure reduces error in the energy predictions by about 7%, and in the force predictions by about 33%. For ANI-Al, we see a much more dramatic improvement: energy and force errors are reduced by about 57% and 88%, respectively. In other words, using force data in the training procedure can reduce force prediction errors by almost a factor of 9.

The biggest difference between the ANI-1x and ANI-Al datasets is that the latter contains DFT calculations

for *bulk* systems (100 to 200 aluminum atoms), whereas the former contains calculations for single molecules only (each with about 15 atoms on average). Consequently, in the ANI-Al dataset, far more information is carried by the force data than the energy data.

## V. CONCLUSIONS

Various works state or imply that training neural network potentials to force data is challenging or expensive. Some studies even opt to ignore forces, and train only to energies. Here, we have discussed two algorithms that make training to force data simple and efficient. With either algorithm, the computational cost of training to energy *and* force data is only a few times more expensive than the cost of training to energy data alone, independent of system size and model complexity. This is striking given that, for a bulk system, the collection of all forces contains vastly more information than does the energy alone.

In Sec. II B we discussed the method of *iterative backpropagation*. Using an ML framework such as PyTorch or TensorFlow, force training can be handled almost automatically. One is free to place arbitrary force-dependent terms into the loss function, and gradients come “for free.” Under the hood, the ML framework traces all intermediate values in the computational graph for calculating the loss function, and will automatically backpropagate through this graph to calculate the gradient of the loss function. We use the term “iterated backpropagation” to refer to the fact backpropagation must happen twice (first to calculate forces and second to calculate the gradient of the loss).

In Sec. IIC we presented a new method that involves taking an appropriate *directional derivative of the energy gradient*. A primary motivation for the new method is that it does not require the use of an ML framework; our method could be applied to *any* existing neural network code that was designed to train to energy data. Compared to iterated backpropagation, the new method requires only half the memory, because it avoids the second backpropagation step. The directional derivative may be estimated with *single* central difference approximation of Eq. (7). The numerical errors associated with finite differencing were found to be negligible in practice. Alternatively, one could in principle retain *full* numerical precision in calculating the loss gradient if the neural network code happens to support a generalization to dual numbers.<sup>5,24</sup>

The benefits of force training have been extensively demonstrated in Ref. 32. Interestingly, that study treats the loss function  $L$  of Eq. (1) in a more approximate way. Namely, the authors reframed the problem in terms of energy training only, by effectively augmenting their dataset with small, random perturbations to existing configurations. Here, in contrast, here we have shown it possible to directly calculate the *full* gradient  $\nabla_{\theta} L$  at

a cost only a few times greater than the cost to calculate  $L$  itself, independent of the system size and the number of model parameters.

We have focused on ML models for which training involves some flavor of gradient descent optimization. Kernel methods, such as Gaussian process regression, are an alternative approach to ML potential development, for which the model parameters are calculated via solution to a linear system of equations.<sup>33,34</sup> Force training is important for kernel models as well as for neural networks.<sup>35,36</sup> One might ask: Could the algorithms presented here also be of use when training kernel models to large quantities of force data?

## ACKNOWLEDGMENTS

This work was partially supported by the Laboratory Directed Research and Development (LDRD) program at LANL. N. L. and A. T. acknowledge support from the Exascale Computing Project (17-SC-20-SC), a collaborative effort of the U.S. Department of Energy Office of Science and the National Nuclear Security Administration. K. B. acknowledges support from the center of Materials Theory as a part of the Computational Materials Science (CMS) program, funded by the U.S. Department of Energy, Office of Science, Basic Energy Sciences, Materials Sciences and Engineering Division. Sandia National Laboratories is a multimission laboratory managed and operated by National Technology & Engineering Solutions of Sandia, LLC, a wholly owned subsidiary of Honeywell International Inc., for the U.S. Department of Energy’s National Nuclear Security Administration under contract de-na0003525. This paper describes objective technical results and analysis. Any subjective views or opinions that might be expressed in the paper do not necessarily represent the views of the U.S. Department of Energy or the United States Government.

## Appendix A: Importance of proper $\eta$ scaling

Figure 1 measured errors in the approximation  $\tilde{\nabla}_\theta L \approx \nabla_\theta L$  for trained and untrained SNAP potentials. By scaling  $\eta$  according to Eqs. (9) and (10), we achieved a good approximator  $\tilde{\nabla}_\theta L$ , valid for both trained and untrained models, using a *single* dimensionless parameter  $\epsilon$ . The invariance of  $\epsilon$  is important because one expects model parameters  $\theta$  to vary significantly over the course of an ML training procedure.

Figure 2 illustrates the danger of naively fixing  $g_0$  constant, rather than using Eq. (10). We observe that, with  $g_0$  fixed, the optimal value of  $\epsilon$  can easily vary by multiple orders of magnitude between trained and untrained models.

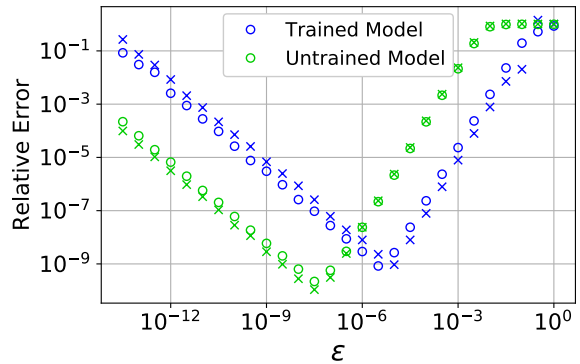


Figure 2. Errors in the finite difference estimates of  $\nabla_\theta L$ , analogous to those of Fig. (1), but here naively fixing  $g_0 = \text{eV}/\text{\AA}$ , rather than using the definition of Eq. (10). With this replacement, the optimal values of  $\epsilon$  now differ significantly between trained and untrained models.

## REFERENCES

- J. S. Smith, B. Nebgen, N. Mathew, J. Chen, N. Lubbers, L. Burakovsky, S. Tretiak, H. A. Nam, T. Germann, S. Fensin, and K. Barros, (2020), arXiv:2003.04934.
- D. Lu, H. Wang, M. Chen, J. Liu, L. Lin, R. Car, W. E. W. Jia, and L. Zhang, (2020), arXiv:2004.11658.
- A. Paszke, S. Gross, F. Massa, A. Lerer, J. Bradbury, G. Chanan, T. Killeen, Z. Lin, N. Gimelshein, L. Antiga, A. Desmaison, A. Kopf, E. Yang, Z. DeVito, M. Raison, A. Tejani, S. Chilamkurthy, B. Steiner, L. Fang, J. Bai, and S. Chintala, in *Advances in Neural Information Processing Systems 32*, edited by H. Wallach, H. Larochelle, A. Beygelzimer, F. d’Alch -Buc, E. Fox, and R. Garnett (Curran Associates, Inc., 2019) pp. 8026–8037.
- M. Abadi, A. Agarwal, P. Barham, E. Brevdo, Z. Chen, C. Citro, G. S. Corrado, A. Davis, J. Dean, M. Devin, S. Ghemawat, I. Goodfellow, A. Harp, G. Irving, M. Isard, Y. Jia, R. Jozefowicz, L. Kaiser, M. Kudlur, J. Levenberg, D. Mane, R. Monga, S. Moore, D. Murray, C. Olah, M. Schuster, J. Shlens, B. Steiner, I. Sutskever, K. Talwar, P. Tucker, V. Vanhoucke, V. Vasudevan, F. Viegas, O. Vinyals, P. Warden, M. Wattenberg, M. Wicke, Y. Yu, and X. Zheng, (2016), arXiv:1603.04467.
- A. Griewank, in *Mathematical Programming: Recent Developments and Applications*, edited by M. Iri and K. Tanabe (Kluwer Academic, Dordrecht, The Netherlands, 1989) pp. 83–108.
- Z. Wang, G.-W. Chern, C. D. Batista, and K. Barros, *J. Chem. Phys.* **148**, 094107 (2018).
- J. Bradbury, R. Frostig, P. Hawkins, M. J. Johnson, C. Leary, D. Maclaurin, and S. Wanderman-Milne, “JAX: Composable transformations of Python+NumPy programs,” (2018).
- S. S. Schoenholz and E. D. Cubuk, (2019), arXiv:1912.04232.
- M. Innes, (2019), arXiv:1810.07951.
- N. Artrith and A. Urban, *Comput. Mater. Sci.* **114**, 135 (2016).
- A. Singraber, (2018), NP2P neural network potential, Available online, <https://compphysvienna.github.io/n2p2/>.
- A. Singraber, T. Morawietz, J. Behler, and C. Dellago, *J. Chem. Theory Comput.* **15**, 3075 (2019).
- J. S. Smith, O. Isayev, and A. E. Roitberg, *Chem. Sci.* **8**, 3192 (2017).
- G. P. P. Pun, R. Batra, R. Ramprasad, and Y. Mishin, *Nat. Commun.* **10**, 2339 (2019).
- N. Lubbers, J. S. Smith, and K. Barros, *J. Chem. Phys.* **148**, 241715 (2018).
- K. T. Sch tt, H. E. Saucedo, P.-J. Kindermans, A. Tkatchenko,

- and K.-R. Müller, *J. Chem. Phys.* **148**, 241722 (2018).
- <sup>17</sup>H. Wang, L. Zhang, J. Han, and W. E, *Comput. Phys. Commun.* **228**, 178 (2018), arXiv:1712.03641.
- <sup>18</sup>K. Yao, J. E. Herr, D. W. Toth, R. Mckintyre, and J. Parkhill, *Chem. Sci.* **9**, 2261 (2018).
- <sup>19</sup>R. Zubatyuk, J. S. Smith, J. Leszczynski, and O. Isayev, *Sci. Adv.* **5**, eaav6490 (2019).
- <sup>20</sup>O. T. Unke and M. Meuwly, *J. Chem. Theory Comput.* **15**, 3678 (2019).
- <sup>21</sup>X. Gao, F. Ramezanghorbani, O. Isayev, J. Smith, and A. Roitberg, (2020), 10.26434/chemrxiv.12218294.v1.
- <sup>22</sup>J. Gilmer, S. S. Schoenholz, P. F. Riley, O. Vinyals, and G. E. Dahl, in *Machine Learning Meets Quantum Physics*, Lecture Notes in Physics, edited by K. T. Schütt, S. Chmiela, O. A. von Lilienfeld, A. Tkatchenko, K. Tsuda, and K.-R. Müller (Springer International Publishing, Cham, 2020) pp. 199–214.
- <sup>23</sup>For efficiency, these gradients should be evaluated using backpropagation. Implementing a *first* iteration of backpropagation manually is not too difficult.
- <sup>24</sup>B. A. Pearlmutter, *Neural Computation* **6**, 147 (1994).
- <sup>25</sup>C. R. Trott, S. D. Hammond, and A. P. Thompson, in *Supercomputing*, Lecture Notes in Computer Science, edited by J. M. Kunkel, T. Ludwig, and H. W. Meuer (Springer International Publishing, Cham, 2014) pp. 19–34.
- <sup>26</sup>A. P. Thompson, L. P. Swiler, C. R. Trott, S. M. Foiles, and G. J. Tucker, *J. Comput. Phys.* **285**, 316 (2015).
- <sup>27</sup>K. He, X. Zhang, S. Ren, and J. Sun, in *Proceedings of the 2015 IEEE International Conference on Computer Vision (ICCV)*, ICCV '15 (IEEE Computer Society, USA, 2015) pp. 1026–1034.
- <sup>28</sup>J. Behler and M. Parrinello, *Phys. Rev. Lett.* **98**, 146401 (2007).
- <sup>29</sup>J. S. Smith, (2020), *Neurochem binaries*, Available online, [https://github.com/isayev/ASE\\_ANI](https://github.com/isayev/ASE_ANI).
- <sup>30</sup>J. S. Smith, R. Zubatyuk, B. Nebgen, N. Lubbers, K. Barros, A. E. Roitberg, O. Isayev, and S. Tretiak, *Sci. Data* **7**, 134 (2020).
- <sup>31</sup>J. S. Smith, B. Nebgen, N. Lubbers, O. Isayev, and A. E. Roitberg, *J. Chem. Phys.* **148**, 241733 (2018).
- <sup>32</sup>A. M. Cooper, J. Kästner, A. Urban, and N. Artrith, *npj Comput. Mater.* **6**, 1 (2020).
- <sup>33</sup>A. P. Bartók and G. Csányi, *International Journal of Quantum Chemistry* **115**, 1051 (2015).
- <sup>34</sup>M. Rupp, *Int. J. Quantum Chem.* **115**, 1058 (2015).
- <sup>35</sup>S. Chmiela, A. Tkatchenko, H. E. Sauceda, I. Poltavsky, K. T. Schütt, and K.-R. Müller, *Sci. Adv.* **3**, e1603015 (2017).
- <sup>36</sup>A. S. Christensen, F. A. Faber, and O. A. von Lilienfeld, *J. Chem. Phys.* **150**, 064105 (2019).